

Synthesis, Structure and Properties of $[\text{Hpy}]_2[\{\text{M}(\text{mnt})_2\}_2]$ (M = Co or Fe, Hpy = pyridinium, mnt = maleonitrile-dithiolate)†

J. Vasco Rodrigues,^a Isabel C. Santos,^a Vasco Gama,^a Rui T. Henriques,^a João C. Waerenborgh,^a M. Teresa Duarte^b and Manuel Almeida^{*a}

^a Departamento de Química, ICEN-INETI, P-2686 Sacavém Codex, Portugal

^b Centro de Química Estrutural, Instituto Superior Técnico, P-1096 Lisboa Codex, Portugal

The compounds $[\text{Hpy}]_2[\{\text{M}(\text{mnt})_2\}_2]$ [M = Fe or Co, Hpy = pyridinium, mnt = maleonitriledithiolate (2,3-disulfanylmaleonitrile)] have been prepared by electrocrystallization and characterized by single-crystal X-ray diffraction, magnetic susceptibility measurements and IR and ⁵⁷Fe Mössbauer spectroscopies. The compounds are isostructural, monoclinic, space group $P2_1/n$ with $Z = 2$. They both consist in alternate packing of $[\{\text{M}(\text{mnt})_2\}_2]^{2-}$ units, with the metal in a square-pyramidal environment co-ordinated by sulfur atoms, and pyridinium cations bridged by three-centred hydrogen bonds to the mnt ligands. Iron-57 Mössbauer spectroscopy confirmed the presence of five-co-ordinate Fe^{III} atoms. Magnetic susceptibility measurements on the cobalt compound showed a small ($\approx 1.5 \times 10^{-4}$ emu mol⁻¹ at room temperature) paramagnetism, almost temperature independent below 150 K ($\approx 0.7 \times 10^{-4}$ emu mol⁻¹), while the iron analogue had a strong paramagnetic contribution of antiferromagnetically coupled pairs of $S = \frac{3}{2}$ in the $[\{\text{Fe}(\text{mnt})_2\}_2]^{2-}$ units, with $-2J/k_B = 515$ K. These properties are correlated to the crystal structure and compared with other $[\{\text{M}(\text{mnt})_2\}_2]^{2-}$ compounds with M = Fe or Co.

Square-planar metal complexes of the type $\text{M}(\text{mnt})_2$, where mnt = maleonitriledithiolate (2,3-disulfanylmaleonitrile) and M is a transition metal (e.g. Pt, Pd, Au, Ni or Cu) have been extensively used in this laboratory as counter ions for conducting molecular solids.¹⁻³ When M = Fe or Co, the $\text{M}(\text{mnt})_2$ units are known to exist as distorted square-pyramidal dimers.^{4,5} For M = Co trimeric⁶ and polymeric⁷ arrangements were found recently in addition to the isolated⁸ and dimeric^{9,10} $\text{Co}(\text{mnt})_2$ units previously known. In this paper we report the synthesis, structure and properties of the pyridinium (Hpy⁺) salts of $[\{\text{Co}(\text{mnt})_2\}_2]^{2-}$ and $[\{\text{Fe}(\text{mnt})_2\}_2]^{2-}$.

Experimental

Synthesis and Electrocrystallization.—Single crystals of $[\text{Hpy}]_2[\{\text{M}(\text{mnt})_2\}_2]$ (M = Fe **1** or Co **2**) were prepared by electrochemical oxidation of $[\text{NBu}_4][\text{M}(\text{mnt})_2(\text{py})]$ in a dichloromethane solution ($\approx 10^{-2}$ mol dm⁻³). The starting compounds $[\text{NBu}_4][\text{M}(\text{mnt})_2(\text{py})]$ (M = Fe or Co) were synthesized as previously reported.¹¹ Dichloromethane (Riedel-deHäen, Chromasolv) was dried with molecular sieves and passed through an alumina column just before use. The solutions were deaerated with argon. Electrocrystallizations were performed in two-compartment cells using platinum electrodes and a galvanostatic oxidation technique¹² (current densities in the range 1.0–1.5 $\mu\text{A cm}^{-2}$). For both complexes **1** and **2** black needle-shaped crystals with a metallic shine and approximate dimensions 4 × 0.5 × 0.5 mm, were collected from the anode compartment after 7 or 10 d and washed with dichloromethane. The crystals were stored under vacuum. Elemental analyses were obtained using a Perkin-Elmer 240 elemental analyser (Found: C, 37.8; H, 1.1; N, 16.7. $\text{C}_{26}\text{H}_{12}\text{Fe}_2\text{N}_{10}\text{S}_8$ requires C, 37.5; H, 1.45; N, 16.8. Found:

C, 37.1; H, 1.2; N, 16.65. $\text{C}_{26}\text{H}_{12}\text{Co}_2\text{N}_{10}\text{S}_8$ requires C, 37.2; H, 1.4; N, 16.7%). Infrared spectra were obtained with a Nicolet 5DXC Fourier-transform infrared spectrometer over the range 4000–200 cm⁻¹ (KBr pellets or Nujol mull); for M = Co: $\tilde{\nu}_{\text{max}}/\text{cm}^{-1}$ 3220–3080m (CH), 2201vs (CN), 1633m, 1597m, 1522m, 1481m, 1440vs, 1383vs, 1233w, 1153s, 1119m, 1046m, 754s, 675s, 609w and 513s; for M = Fe: $\tilde{\nu}_{\text{max}}/\text{cm}^{-1}$ 3220–3080m (CH), 2208vs (CN), 1633m, 1593m, 1522s, 1480s, 1232w, 1147w, 1111vw, 1045w, 753s, 674s, 609vw, 509s and 378s.

X-Ray Crystallography.— $[\text{Hpy}]_2[\{\text{Fe}(\text{mnt})_2\}_2]$ **1**. A black crystal of approximate dimensions 1 × 0.1 × 0.1 mm was sealed in a glass capillary and mounted on a goniometer head. X-Ray data were collected on an Enraf-Nonius FAST diffractometer with a Nonius FR571 rotating anode generator (50 kV and 60 mA) and an apparent spot size of 0.3 × 0.3 mm. Intensity data measurements were carried out using SADNES, a modified version of the MADNES¹³ software, for small molecule data collection. The crystal to detector distance was set to 45 mm and a detector tilt angle of $\theta = 26^\circ$ was used. In addition, an exposure time of 15 s per 0.25° frame was used throughout. In order to achieve a unique data set as complete as possible, six separate measurements were carried out. For each measurement reflection profiles were extracted on-line from the integrated mass store images. Data reduction for each measurement was later carried out by the Kabsch profile-fitting method using PROCOR,¹⁴ which produced a file containing intensities corrected for Lorentz and polarization effects, and internally scaled together on the basis of the intensities of symmetry equivalent reflections. The intensities from the six measurements were then scaled and merged together using SHELX 76.^{15a} The initial values of the cell parameters were determined by an autoindexing procedure applied to 50 intense reflections covering two narrow (ca. 5° wide) and nearly orthogonal regions of reciprocal space. Throughout the data collection process the cell parameters were refined together with the orientation matrix every 10 of measured data.

$[\text{Hpy}]_2[\{\text{Co}(\text{mnt})_2\}_2]$ **2**. A black crystal of approximate

† Supplementary data available: see Instructions for Authors, *J. Chem. Soc., Dalton Trans.*, 1994, Issue 1, pp. xxiii–xxviii.

Non-SI unit employed: emu = SI × 10⁶/4π.

dimensions $1 \times 0.1 \times 0.1$ mm was sealed in a glass capillary and mounted on a goniometer head. X-Ray data were collected on an Enraf-Nonius TURBO CAD-4 diffractometer with a Nonius FR571 rotating anode generator (50 kV and 80 mA). Unit-cell dimensions and their standard deviations were determined from 25 reflections in the range $12 < \theta < 16^\circ$. The data were corrected for Lorentz, polarization and absorption effects (maximum and minimum transmission factors 0.99 and 0.98). Crystallographic details are summarized in Table 1.

Structure solution and refinement. Intensity data for both compounds **1** and **2** were consistent with space group $P2_1/n$. The structures of both compounds were solved by direct methods using SHELX 86;^{15b} the remaining atoms were located from successive Fourier difference maps and included in subsequent calculations. Least-squares refinements were carried out using SHELX 76.^{15a} All the non-hydrogen atoms were

refined anisotropically and the hydrogen atoms isotropically. The final refinements were carried out with the weighting scheme $w = 1.0/[\sigma^2(F_o) + 0.0001F_o^2]$. Atomic scattering factors were taken from ref. 16. The final fractional atomic coordinates of the non-hydrogen atoms are listed in Table 2 and selected bond lengths and angles in Tables 3 and 4. All calculations were carried out on a VAX 9000 computer at the Instituto Superior Técnico, using SHELX,¹⁵ PARST¹⁷ (calculation of geometric data) and ORTEP II¹⁸.

Additional material available from the Cambridge Crystallographic Data Centre comprises H-atom coordinates, thermal parameters and remaining bond lengths and angles.

Mössbauer Spectroscopy.—Mössbauer absorbers (≈ 0.40 mg of natural Fe per cm^2) were prepared by stacking needle-shaped single crystals of $[\text{Hpy}]_2[\{\text{Fe}(\text{mnt})_2\}_2]$ **1** into a Perspex holder. Mössbauer spectra were measured in the transmission mode using a source of ^{57}Co in Rh (≈ 20 mCi). The velocity wave had a symmetric 'saw-tooth' shape, and the spectrometer was calibrated against an Fe foil absorber. Spectra were obtained

Table 1 Crystal data and details of structure determination for complexes **1** and **2**

	1	2
Formula	$\text{C}_{13}\text{H}_6\text{FeN}_5\text{S}_4$	$\text{C}_{13}\text{H}_6\text{CoN}_5\text{S}_4$
<i>M</i>	416.344	419.424
Crystal system	Monoclinic	Monoclinic
Space group	$P2_1/n$	$P2_1/n$
<i>a</i> /Å	16.080(5)	16.131(2)
<i>b</i> /Å	6.268(2)	6.277(1)
<i>c</i> /Å	17.602(2)	17.572(2)
β /°	115.35(2)	117.04(1)
<i>U</i> /Å ³	1603.28(64)	1584.92(37)
<i>D_c</i> /g cm ⁻³	1.725	1.754
<i>F</i> (000)	832	836
$\mu(\text{Mo-K}\alpha)/\text{mm}^{-1}$	1.35	1.59
<i>R</i> _{int}	—	0.0126
Unique reflections	3963	3319
Reflections used [$F_o > 3\sigma(F_o)$]	2384	2573
$\Delta/\sigma(\text{maximum})$	0.063	0.075
Residual density/e Å ⁻³	0.88	0.52
<i>R</i> ^a	0.0752	0.0463
<i>R</i> ^b	0.0636	0.0348

Details in common: *Z* = 4; $\lambda(\text{Mo-K}\alpha) = 0.71069$ Å; *h, k, l* range -21 to 0, -8 to 0, -23 to 23 ($3 < 2\theta < 56^\circ$); parameters refined, 232. ^a $R = \Sigma(|F_o| - |F_c|)/\Sigma|F_o|$. ^b $R' = [\Sigma w(|F_o| - |F_c|)^2/\Sigma w|F_o|^2]^{1/2}$.

Table 3 Selected bond lengths (Å) for $[\text{Hpy}]_2[\{\text{M}(\text{mnt})_2\}_2]$ (*M* = Fe **1** or Co **2**)

<i>M</i> (mnt) ₂ ⁻ unit	1		2		
	1	2	1	2	
M-M(a)	3.064(1)	3.147(1)	S(1)-M(a)	2.493(2)	2.429(1)
S(1)-M	2.235(4)	2.188(3)	S(2)-M	2.218(4)	2.184(3)
S(3)-M	2.223(4)	2.185(3)	S(4)-M	2.230(4)	2.186(3)
C(1)-S(1)	1.749(8)	1.738(5)	C(2)-S(2)	1.726(8)	1.704(6)
C(3)-S(3)	1.731(9)	1.713(6)	C(4)-S(4)	1.758(9)	1.718(6)
C(2)-C(1)	1.352(9)	1.363(6)	C(6)-C(1)	1.420(9)	1.421(6)
C(5)-C(2)	1.446(9)	1.439(6)	C(4)-C(3)	1.345(10)	1.376(6)
C(7)-C(3)	1.421(10)	1.433(7)	C(8)-C(4)	1.443(10)	1.439(6)
N(1)-C(5)	1.135(9)	1.137(5)	N(2)-C(6)	1.149(9)	1.145(6)
N(3)-C(7)	1.153(9)	1.138(6)	N(4)-C(8)	1.126(9)	1.135(6)
Hpy ⁺ unit					
C(11)-N	1.330(10)	1.337(7)	C(15)-N	1.326(11)	1.337(7)
C(12)-C(11)	1.370(11)	1.366(7)	C(13)-C(12)	1.376(12)	1.367(8)
C(13)-C(14)	1.363(12)	1.359(8)	C(15)-C(14)	1.354(12)	1.363(8)

Symmetry operator (a) $-x, -y, -z$.

Table 2 Fractional atomic coordinates ($\times 10^4$)

Atom	$[\text{Hpy}]_2[\{\text{Fe}(\text{mnt})_2\}_2]$			$[\text{Hpy}]_2[\{\text{Co}(\text{mnt})_2\}_2]$		
	<i>x</i>	<i>y</i>	<i>z</i>	<i>x</i>	<i>y</i>	<i>z</i>
M	925(1)	549(1)	-8(1)	978	442(1)	37
S(1)	588(1)	-2412(2)	511(1)	501(1)	-2305(2)	498(1)
S(2)	1590(1)	1924(3)	1275(1)	1585(1)	1890(2)	1306(1)
S(3)	1645(1)	3058(3)	-393(1)	1615(1)	3006(2)	-358(1)
S(4)	772(1)	-1386(3)	-1123(1)	790(1)	-1484(2)	-1066(1)
C(1)	1027(5)	-1900(10)	1590(4)	994(3)	-1889(6)	1595(2)
C(2)	1439(4)	-13(10)	1902(4)	1427(3)	-3(6)	1923(2)
C(3)	1425(5)	2339(10)	-1411(4)	1387(3)	2262(7)	-1372(2)
C(4)	1022(5)	473(11)	-1745(4)	1002(3)	308(6)	-1696(2)
C(5)	1688(5)	562(10)	2768(4)	1695(3)	555(7)	2798(2)
C(6)	896(5)	-3460(10)	2114(4)	861(3)	-3439(6)	2119(2)
C(7)	1693(5)	3825(10)	-1875(4)	1642(3)	3739(7)	-1851(3)
C(8)	771(5)	-74(10)	-2612(4)	751(3)	-224(7)	-2570(3)
N(1)	1842(5)	1064(9)	3435(4)	1870(3)	1066(6)	3475(2)
N(2)	780(5)	-4636(9)	2560(4)	771(3)	-4643(6)	2566(2)
N(3)	1944(5)	5038(11)	-2223(4)	1890(3)	4931(7)	-2191(3)
N(4)	535(5)	-445(11)	-3299(4)	512(3)	-574(7)	-3273(2)
N	3730(5)	-597(10)	668(4)	3755(3)	-601(6)	675(2)
C(11)	3335(6)	-1810(12)	-13(5)	3344(3)	-1807(8)	-26(3)
C(12)	3305(6)	-1125(13)	-764(5)	3313(4)	-1121(8)	-777(3)
C(13)	3702(6)	805(13)	-786(5)	3690(3)	807(8)	-808(3)
C(14)	4099(6)	2006(13)	-75(5)	4097(4)	2023(9)	-92(3)
C(15)	4114(7)	1266(14)	654(5)	4126(4)	1285(9)	649(3)

with the absorbers at 300 and 80 ± 1 K using a helium flow cryostat. Computer fitting of the data was performed on folded spectra assuming doublets of Lorentzian line shape and using a non-linear least-squares method.¹⁹

Magnetic Susceptibility.—Magnetic susceptibility measurements were performed in the ranges 20–300 K for complex **1** and 5–300 K for **2**, using a Faraday system (Oxford Instruments) with a 7 T superconducting magnet on polycrystalline samples (≈ 8 mg for **1** and ≈ 6 mg for **2**) placed in a thin-walled Teflon bucket. The magnetic field used was 5 T, and the force was measured with a microbalance (Sartorius S3D-V) applying forward and reverse gradients of 5 T m^{-1} . Under these conditions the magnetization was found to be proportional to the applied magnetic field.

Results and Discussion

The compounds $[\text{Hpy}]_2[\text{M}(\text{mnt})_2]_2$ ($\text{M} = \text{Fe}$ **1** or Co **2**) are isostructural. The asymmetric unit comprises one $\text{M}(\text{mnt})_2^-$ anion and one Hpy^+ cation. The crystal structures consist of mixed stacks of $\text{M}(\text{mnt})_2^-$ dimers alternating with pairs of pyridinium molecules along the b axis (Fig. 1). The result is the existence of discrete dimers related by an inversion centre located between the two metal atoms. The two $\text{M}(\text{mnt})_2^-$ units are in a staggered conformation such that the metal atom of one unit sits 2.429(1) (**2**) or 2.493(2) Å (**1**) above a sulfur atom from the other unit of the dimer. The metal atom has a distorted square-pyramidal co-ordination geometry and is displaced by 0.36 (**1**) or 0.23 Å (**2**) from the least-squares plane defined by the

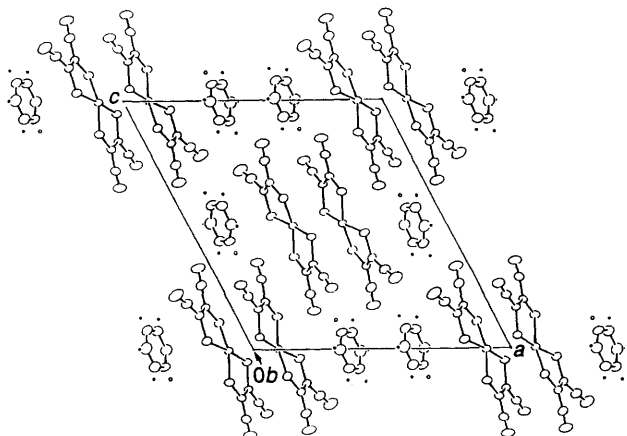


Fig. 1 Projection of $[\text{Hpy}]_2[\text{Co}(\text{mnt})_2]_2$ along the b axis

four sulfur atoms of the basal ligand (Fig. 2). The dihedral angle between the $\text{MS}(1)\text{S}(2)$ and $\text{MS}(3)\text{S}(4)$ planes is $29.87(9)^\circ$ for **1** and $19.10(5)^\circ$ for **2**. These dimeric arrangements, with the metal in a square-pyramidal co-ordination geometry, are similar to those previously found in other bis(1,2-dithiolene) complexes²⁰ and virtually identical to those of $[\text{NBu}_4]_2[\text{Co}(\text{mnt})_2]_2$ ²¹ and $[\text{NBu}_4]_2[\text{Fe}(\text{mnt})_2]_2$.⁴ Within experimental uncertainty the pyridine rings are planar with an average deviation of 0.0036 Å in **1** and 0.0031 Å in **2**. In both cases, the interplanar distance between adjacent pyridine rings, 3.60 and 3.57 Å for compounds **1** and **2** respectively, are well above the van der Waals contact distances (≈ 3.40 Å). In both structures, the cations are almost parallel to the average plane of a $\text{M}(\text{mnt})_2^-$ unit with a dihedral angle between the best planes of $\approx 5^\circ$. Although the hydrogens could not be located accurately by X-ray diffraction it should be noted that in both compounds and as shown for compound **2** in Fig. 3, the distances between the pyridine nitrogen (N) and the nitrogens of the mnt ligands of two different $\text{M}(\text{mnt})_2^-$ units [N(1a) and N(2b)] are compatible with the existence of three-centred hydrogen bonds (Table 5). Other possible hydrogen bonds are included in Table 5.

The existence of protonated pyridine could not be concluded from the IR spectra of compounds **1** and **2**. The N^+-H

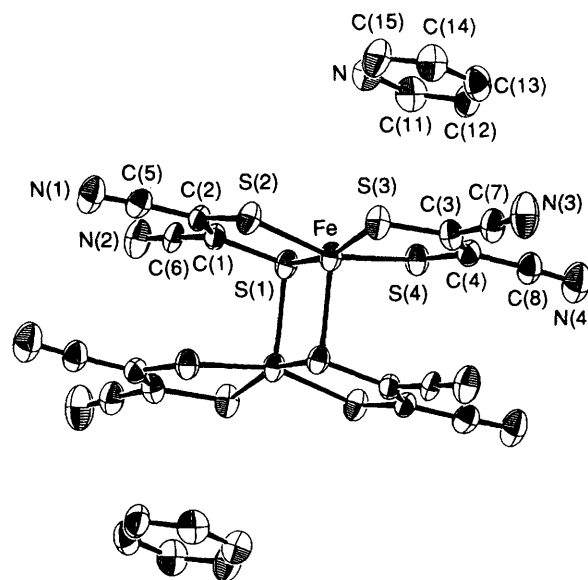


Fig. 2 ORTEP view of the $[\text{Fe}(\text{mnt})_2]_2^{2-}$ dimer and two pyridine rings with the atom numbering scheme used

Table 4 Selected bond angles ($^\circ$) for $[\text{Hpy}]_2[\text{M}(\text{mnt})_2]_2$ ($\text{M} = \text{Fe}$ **1** or Co **2**)

$\text{M}(\text{mnt})_2^-$ unit	1	2		1	2
$\text{S}(2)-\text{M}-\text{S}(1)$	90.12(2)	91.7(4)	$\text{S}(3)-\text{M}-\text{S}(1)$	163.94(1)	173.29(6)
$\text{S}(3)-\text{M}-\text{S}(2)$	87.03(2)	87.71(5)	$\text{S}(4)-\text{M}-\text{S}(1)$	87.41(2)	87.82(4)
$\text{S}(4)-\text{M}-\text{S}(2)$	158.64(1)	162.29(6)	$\text{S}(4)-\text{M}-\text{S}(3)$	89.53(2)	91.35(5)
$\text{C}(1)-\text{S}(1)-\text{M}$	103.6(3)	103.4(2)	$\text{C}(2)-\text{S}(2)-\text{M}$	103.9(3)	103.4(2)
$\text{C}(3)-\text{S}(3)-\text{M}$	103.3(3)	102.7(2)	$\text{C}(4)-\text{S}(4)-\text{M}$	102.6(3)	102.8(2)
$\text{C}(2)-\text{C}(1)-\text{S}(1)$	120.1(6)	119.2(4)	$\text{C}(6)-\text{C}(1)-\text{S}(1)$	118.4(6)	119.2(4)
$\text{C}(6)-\text{C}(1)-\text{C}(2)$	121.4(7)	121.4(4)	$\text{C}(1)-\text{C}(2)-\text{S}(2)$	122.2(6)	122.2(4)
$\text{C}(5)-\text{C}(2)-\text{S}(2)$	116.6(6)	116.8(4)	$\text{C}(5)-\text{C}(2)-\text{C}(1)$	120.9(7)	120.7(4)
$\text{C}(4)-\text{C}(3)-\text{S}(3)$	121.7(6)	121.1(4)	$\text{C}(7)-\text{C}(3)-\text{S}(3)$	116.5(6)	116.9(4)
$\text{C}(7)-\text{C}(3)-\text{C}(4)$	121.9(7)	122.0(5)	$\text{C}(3)-\text{C}(4)-\text{S}(4)$	120.1(6)	120.1(4)
$\text{C}(8)-\text{C}(4)-\text{S}(4)$	117.8(6)	119.6(4)	$\text{C}(8)-\text{C}(4)-\text{C}(3)$	122.2(7)	120.2(5)
$\text{N}(1)-\text{C}(5)-\text{C}(2)$	176.6(7)	176.5(4)	$\text{N}(2)-\text{C}(6)-\text{C}(1)$	176.4(7)	177.6(4)
$\text{N}(3)-\text{C}(7)-\text{C}(3)$	177.2(9)	176.2(5)	$\text{N}(4)-\text{C}(8)-\text{C}(4)$	176.5(8)	176.3(5)
Hpy⁺ unit					
$\text{C}(15)-\text{N}-\text{C}(11)$	122.3(8)	120.8(5)	$\text{C}(12)-\text{C}(11)-\text{N}$	119.7(8)	119.8(6)
$\text{C}(13)-\text{C}(12)-\text{C}(11)$	118.6(9)	119.8(6)	$\text{C}(15)-\text{C}(14)-\text{C}(13)$	119.5(9)	119.1(9)
$\text{C}(14)-\text{C}(13)-\text{C}(12)$	120.0(8)	119.8(6)	$\text{C}(14)-\text{C}(15)-\text{N}$	120.0(9)	120.8(6)

Table 5 Distances (Å) and angles (°) for possible hydrogen bonds in [Hpy]₂[{M(mnt)₂}] (M = Fe 1 or Co 2)

Donor...acceptor	1	2	H...acceptor	1	2	Donor-H...acceptor	1	2
N...N(1a)	2.994(11)	3.022(6)	H...N(1a)	2.146(89)	2.425(60)	N-H...N(1a)	138.57(6.30)	134.02(4.63)
N...N(2b)	2.935(9)	2.911(5)	H...N(2b)	2.209(82)	2.275(55)	N-H...N(2b)	126.26(6.03)	138.78(5.16)
C(11)...N(1a)	3.202(12)	3.199(7)	H(1)...N(1a)	2.771(65)	2.656(48)	C(11)-H(1)...N(1a)	114.81(4.39)	118.06(3.06)
C(15)...N(2b)	3.127(12)	3.129(7)	H(5)...N(2b)	2.583(83)	2.628(56)	C(15)-H(5)...N(2b)	119.28(5.24)	116.02(3.65)
C(13)...N(3c)	3.236(12)	3.243(7)	H(3)...N(3c)	2.504(93)	2.528(45)	C(13)-H(3)...N(3c)	132.19(7.03)	134.94(3.62)
C(13)...N(4d)	3.367(13)	3.363(8)	H(3)...N(4d)	2.589(101)	2.628(50)	C(13)-H(3)...N(4d)	137.16(7.08)	137.51(3.45)

Symmetry operations (a) $0.5 - x, -0.5 + y, 0.5 - z$; (b) $0.5 - x, 0.5 + y, 0.5 - z$; (c) $0.5 - x, -0.5 + y, -0.5 - z$; (d) $0.5 - x, 0.5 + y, -0.5 - z$.

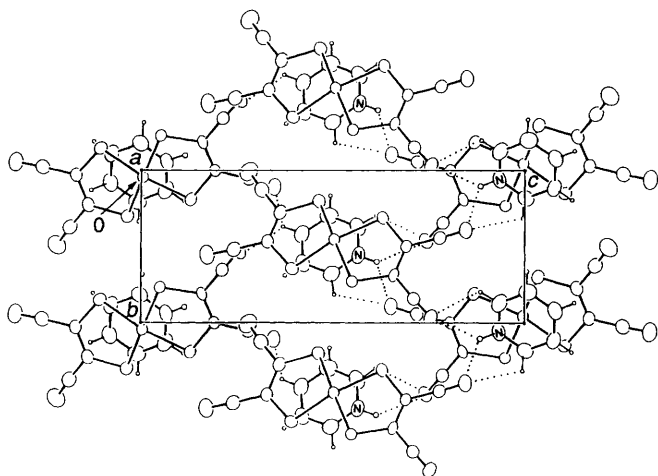


Fig. 3 Partial projection of [Hpy]₂[{Co(mnt)₂}]₂ **2** along the *a* axis, illustrating the possible hydrogen bonds. For simplicity only NH...N(1a), NH...N(2b), C(11)H...N(1a) and C(15)H...N(2b) bonds (Table 5) are shown for one pyridinium and the corresponding Co(mnt)₂ unit. Hydrogen bonds therefore also exist for the other units generated by an inversion centre

vibrational band, which would be expected to occur in the range 2500–2325 cm⁻¹ (ref. 22), was not observed. Either this band is too broad or it lies under the strong C≡N stretching vibration at ≈2200 cm⁻¹. In both cases, the C–H stretching bands of the pyridine ring are observed in the usual range of 3220–3080 cm⁻¹. In spite of the absence of IR evidence for Hpy⁺, the existence of pyridine radical cations is hardly conceivable. Pyridine radical cations are unstable and well separated pyridine radicals, as in the present structures, would give an extra contribution to the magnetic susceptibility not observed experimentally (see later). The likely presence of Hpy⁺ requires, during the electrochemical oxidation, a reaction with a proton source, either the solvent itself or traces of water. It should be noted that attempts to prepare these compounds by the direct reaction of [Hpy]Br and Na₂[{M(mnt)₂}]₂ gave, M = Fe only, black plate-shaped crystals but with different structural parameters and elemental analysis (C, 42.8; H, 1.9; N, 16.7%), suggesting three pyridines for two Fe(mnt)₂ units.²³

All the Mössbauer spectra were fitted with one quadrupole doublet (Fig. 4). For [Hpy]₂[{Fe(mnt)₂}]₂ **1** both peaks have the same width but different areas (Fig. 4); this may be attributed to texture effects. The estimated parameters are summarized in Table 6 together with published values for [(per)₂]₂[{Fe(mnt)₂}]₂ [where (per)₂ represents two perylene molecules with an overall charge of +1],²⁴ [NBu₄]₂[{Fe(mnt)₂}]₂^{24,25} and [NEt₄]₂[{Fe(mnt)₂}]₂.²⁶ Within experimental error, the parameters are the same for the pyridinium, perylene and tetraalkylammonium compounds, the quadrupole splitting, Δ, values for the pyridinium and tetrabutylammonium compounds being slightly lower than the others. The isomer shift values are compatible with Fe^{III} in a square-pyramidal configuration. The low half-width, Γ, values

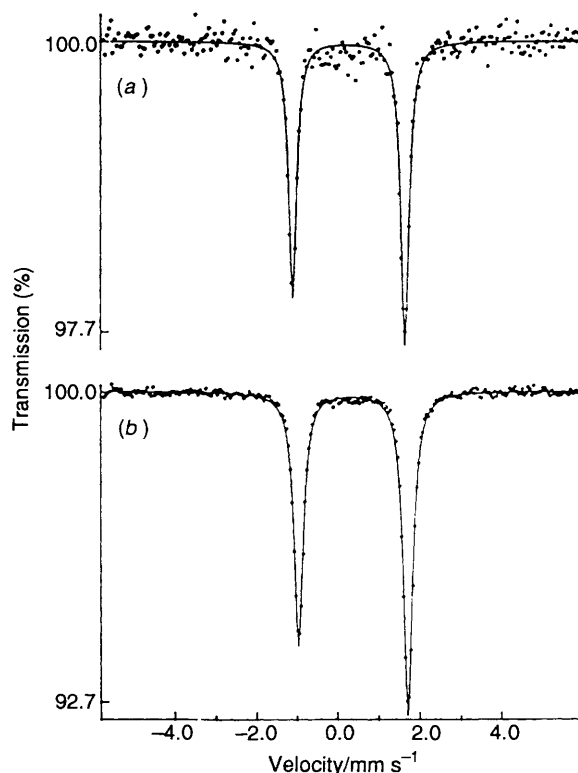


Fig. 4 Iron-57 Mössbauer spectra of [Hpy]₂[{Fe(mnt)₂}]₂ **1** at (a) 300 and (b) 80 K

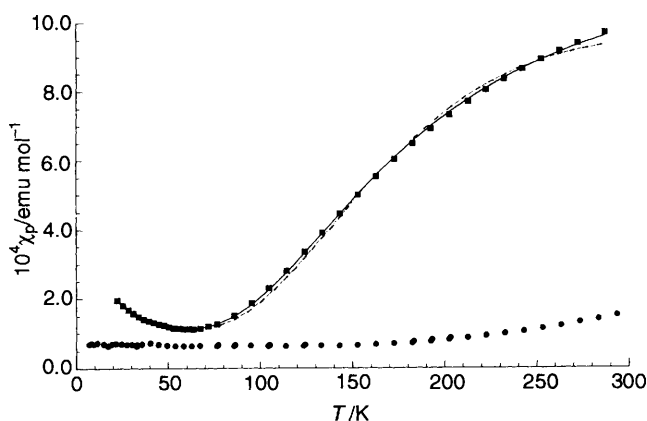


Fig. 5 Paramagnetic susceptibility of [Hpy]₂[{M(mnt)₂}]₂ [M = Fe **1** (■) or Co **2** (●)] as a function of temperature. The solid line represents the fit of equations (2) and (3); the dashed line corresponds to the fit of equations (1) and (3)

are consistent with only one kind of environment for the iron atom. The increase in the isomer shift as the temperature is lowered is a result of the second-order Doppler effect.

Table 6 Mössbauer data obtained at different temperatures*

Absorber	T/K	δ / mm s ⁻¹	Δ / mm s ⁻¹	Γ / mm s ⁻¹	Ref.
[Hpy] ₂ [{Fe(mnt) ₂ }] ₂	300	0.24	2.75	0.24	This work
	80	0.35	2.69	0.28	This work
[(per) ₂] ₂ [{Fe(mnt) ₂ }] ₂	295	0.25	2.83	0.26	24
	80	0.34	2.79	0.28	24
	15	0.36	2.79	0.25	24
[NBu ₄] ₂ [{Fe(mnt) ₂ }] ₂	295	0.23			25
	80	0.33	2.68	0.29	24
[NEt ₄] ₂ [{Fe(mnt) ₂ }] ₂	295	0.24	2.81		26
	77	0.33	2.76		26

* δ = isomer shift relative to metallic iron; Δ = quadrupole splitting; Γ = full width at half height. Precision in the fitting procedure: ± 0.01 mm s⁻¹ for δ , Δ and Γ .

Table 7 Paramagnetic susceptibility data^a

Compound	10 ⁻⁴ C/K emu mol ⁻¹	C'/K emu mol ⁻¹	-2J/ k _B ^b	Ref.
[Hpy] ₂ [{Fe(mnt) ₂ }] ₂	31	2.065	515	This work
[(per) ₂] ₂ [{Fe(mnt) ₂ }] ₂	89	1.342	300	24
[NBu ₄] ₂ [{Fe(mnt) ₂ }] ₂	310	1.579	394	24
[NEt ₄] ₂ [{Fe(mnt) ₂ }] ₂	227	1.661	374	24

^a C = Curie constant, C' = $Ng^2\mu_B^2/k_B$. ^b In units of K; J = exchange coupling constant.

Paramagnetic molar susceptibility, χ_p , results obtained from magnetization measurements on crystals of [Hpy]₂[{Co(mnt)₂}]₂ **2**, in the range 5–300 K and after correction for a diamagnetic contribution estimated from Pascal constants of -1.75×10^{-4} emu mol⁻¹, are shown in Fig. 5. At room temperature, the paramagnetic susceptibility is 1.5×10^{-4} emu mol⁻¹, which decreases slightly upon cooling until 150 K and reaches a temperature independent value of 0.7×10^{-4} emu mol⁻¹, with no noticeable Curie tail down to 5 K. This small value can partially reflect an experimental error or, most probably is the result of a temperature-independent paramagnetic contribution from the [{Co(mnt)₂}]₂²⁻ units. In this respect it is noteworthy that a similar value of a residual paramagnetism, 0.7×10^{-4} emu mol⁻¹, was found in this laboratory for [(per)₂]₂[{Co(mnt)₂}]₂ at lower temperatures,²⁴ where a diamagnetic state is expected, thus also supporting the existence of a temperature-independent paramagnetism in the Co(mnt)₂⁻ units.

Paramagnetic molar susceptibility values obtained from magnetization measurements of [Hpy]₂[{Fe(mnt)₂}]₂ **1** are also shown in Fig. 5, after correction for a diamagnetic contribution estimated from Pascal constants of -1.75×10^{-4} emu mol⁻¹. At low temperature the results are dominated by a Curie tail due to impurities and/or defects. As previously observed in other compounds with dimerised Fe(mnt)₂⁻ units,²⁴ the contribution from the Fe(mnt)₂⁻ units to the magnetic susceptibility is expected to result from antiferromagnetically coupled pairs of spins in dimers with an exchange coupling constant J and, at least in a first approximation, with negligible interdimer interactions. This contribution depends on the total spin S in each Fe(mnt)₂⁻ unit: if $S = \frac{1}{2}$, the interaction is given by²⁷ equation (1), where g is the effective average

$$\chi_{Fe}(s = \frac{1}{2}) = \frac{Ng^2\mu_B^2}{k_B T} \left[3 + \exp(-2J/k_B T) \right]^{-1} \quad (1)$$

splitting factor (Landé constant), μ_B is the Bohr magneton, N Avogadro's number and T the absolute temperature. However, if $S = \frac{3}{2}$, the contribution follows²⁷ equation (2). The results of

$$\chi_{Fe}(s = \frac{3}{2}) = \frac{Ng^2\mu_B^2}{k_B T} \times \left[\frac{\exp(2J/k_B T) + 5 \cdot \exp(6J/k_B T) + 14 \cdot \exp(12J/k_B T)}{1 + 3 \cdot \exp(2J/k_B T) + 5 \cdot \exp(6J/k_B T) + 7 \cdot \exp(12J/k_B T)} \right] \quad (2)$$

the paramagnetic molar susceptibility of [Hpy]₂[{Fe(mnt)₂}]₂, χ_p , were fitted by expression (3), where A is a temperature-

$$\chi_p = A + \chi_{imp} + \chi_{Fe} \quad (3)$$

independent contribution, $\chi_{imp} = C/T$ is the impurity susceptibility and χ_{Fe} the contribution of the dimer. For χ_{Fe} either equation (1) or (2) was used. A closer agreement between the observed and calculated paramagnetic susceptibility was obtained when using equations (2) and (3), with $A = 5.7 \times 10^{-5}$ emu mol⁻¹, $C = 30.9 \times 10^{-4}$ K emu mol⁻¹, $C' = (Ng^2\mu_B^2)/k_B = 2.065$ K emu mol⁻¹ and $-2J/k_B = 515$ K, as shown by the solid line in Fig. 5. A poorer fit was obtained with equations (1) and (3) (dashed line in Fig. 5), confirming that Fe(mnt)₂⁻, in this compound, is in a $S = \frac{3}{2}$ spin configuration, as already observed²⁴ for other compounds with dimers of distorted square pyramids such as [(per)₂]₂[{Fe(mnt)₂}]₂, [NEt₄]₂[{Fe(mnt)₂}]₂ and [NBu₄]₂[{Fe(mnt)₂}]₂.

The fitting parameters are compared in Table 7 with those previously published for similar compounds. The temperature independent contribution A is quite small, about 80% of that found for the Co analogue **1**. The C value corresponds to $\approx 0.8\%$ of $S = \frac{1}{2}$ impurities (or 0.2% of $S = \frac{3}{2}$).

As shown in Table 7, the main difference between [Hpy]₂[{Fe(mnt)₂}]₂ and the other dimerised Fe(mnt)₂⁻ compounds is the larger J value. This difference contrasts with the almost identical structural parameters derived from X-ray diffraction and the equally similar Mössbauer parameters (Table 6). Therefore it is clear that the different J values in the [{Fe(mnt)₂}]₂²⁻ compounds do not reflect different dimeric structures but instead they should be regarded as a result of different interdimer interactions that were neglected in equation (2). In fact, in [Hpy]₂[{Fe(mnt)₂}]₂ the dimers are well separated by the Hpy⁺ cations without any significant interdimer M–S contact, while in the tetrabutylammonium and perylene compounds the dimers are stacked.^{24,25} These dimers are stacked in a staggered way in the tetrabutylammonium compound²⁵ while in the perylene compound, as judged by the average structure,²⁴ they are eclipsed enabling an even closer interdimer M–S contact. This provides a good correlation of the decreasing effective J value obtained from equation (2), with the increasing interdimer interaction.

Acknowledgements

This work was partially supported by the Junta Nacional de Investigação Científica e Tecnológica (Portugal) under contracts PCMT/C/PMF/798/90 and PBIC/C/CEN1157/92.

References

- R. T. Henriques, V. Gama, G. Bonfait, I. C. Santos, M. J. Matos, M. Almeida, M. T. Duarte and L. Alcácer, *Synth. Metals*, 1993, **55–57**, 1846.
- V. Gama, R. T. Henriques, G. Bonfait, M. Almeida, S. Ravy, J. P. Pouget and L. Alcácer, *Mol. Cryst. Liq. Cryst.*, 1993, **234**, 171.
- M. Almeida, V. Gama, R. T. Henriques and L. Alcácer, in *Inorganic and Organometallic Polymers with Special Properties*, ed. R. M. Laine, Kluwer, Dordrecht, 1993, pp. 163–177.
- W. C. Hamilton and I. Bernal, *Inorg. Chem.*, 1967, **6**, 2003.
- A. L. Balch, I. G. Dance and R. H. Holm, *J. Am. Chem. Soc.*, 1968, **90**, 1139.
- V. Gama, R. T. Henriques, M. Almeida, L. Veiros, M. J. Calhorda, A. Meetsma and J. L. de Boer, *Inorg. Chem.*, 1993, **32**, 3705.
- V. Gama, R. T. Henriques, G. Bonfait, M. Almeida, A. Meetsma, S. van Smaalen and J. L. de Boer, *J. Am. Chem. Soc.*, 1992, **114**, 1986.

- 8 J. D. Forrester, A. Zalkin and D. H. Templeton, *Inorg. Chem.*, 1964, **3**, 1500.
- 9 M. J. Baker-Hawkes, Z. Dori, R. Eisenberg and H. B. Gray, *J. Am. Chem. Soc.*, 1968, **90**, 4253.
- 10 J. H. Enemark and W. N. Lipscomb, *Inorg. Chem.*, 1965, **4**, 1729.
- 11 I. G. Dance and T. R. Miller, *Inorg. Chem.*, 1974, **13**, 525.
- 12 E. M. Engler, R. Green, P. Haen, Y. Tomkiewicz, K. Mortensen and J. Berendzen, *Mol. Cryst. Liq. Cryst.*, 1982, **79**, 15.
- 13 A. Messerschmidt and J. W. Pflugrath, *J. Appl. Crystallogr.*, 1987, **20**, 306.
- 14 J. W. Pflugrath and A. Messerschmidt, *Crystallography in Molecular Biology*, Meeting Abstracts, Bischenberg, France, 1985.
- 15 (a) G. M. Sheldrick, SHELX 76, Program for Crystal Structure Determination, University of Cambridge, 1976; (b) G. M. Sheldrick, SHELX 86, Program for Crystal Structure Solution, University of Göttingen, 1986.
- 16 *International Tables for X-Ray Crystallography*, Kynoch Press, Birmingham, 1974, vol. 4.
- 17 M. Nardelli, *Comput. Chem.*, 1983, **7**, 95.
- 18 C. K. Johnson, ORTEP II, Report ORNL-3138, Oak Ridge National Laboratory, TN, 1976.
- 19 A. J. Stone, in G. M. Bancroft, A. G. Maddock, W. K. Ong, R. H. Prince and A. J. Stone, *J. Chem. Soc. A*, 1967, 1966 (appendix).
- 20 D. Buckingham and C. R. Clark, in *Comprehensive Coordination Chemistry*, eds. G. Wilkinson, R. Gillard and J. McCleverty, Pergamon Press, Oxford, 1987, vol. 4, p. 874.
- 21 I. C. Santos and M. T. Duarte, unpublished work.
- 22 L. J. Bellamy, *The Infrared Spectra of Complex Molecules*, Chapman and Hall, London, 3rd edn., 1975.
- 23 J. V. Rodrigues, I. C. Santos and M. Almeida, unpublished work.
- 24 V. Gama, R. T. Henriques, G. Bonfait, L. C. Pereira, J. C. Waerenborgh, I. C. Santos, M. T. Duarte, J. M. P. Cabral and M. Almeida, *Inorg. Chem.*, 1992, **31**, 2600.
- 25 T. Birchall and N. N. Greenwood, *J. Chem. Soc. A*, 1969, 286.
- 26 J. L. K. F. De Vries, M. Trooster and E. de Boer, *Inorg. Chem.*, 1971, **10**, 81.
- 27 R. L. Carlin, *Magnetochemistry*, Springer-Verlag, Berlin, 1986, pp. 75, 94.

Received 26th April 1994; Paper 4/02464H